Multi-timescale Modeling of Fast Charging Stations for Power Quality Analysis

Wang, Lu; Qin, Zian; Beloqui Larumbe, Lucia; Bauer, Pavol

Publication date
2021

Document Version
Accepted author manuscript

Published in
2021 23rd European Conference on Power Electronics and Applications (EPE'21 ECCE Europe)

Multi-timescale Modeling of Fast Charging Stations for Power Quality Analysis

Lu Wang, Zian Qin, Lucia Beloqui Larumbe, Pavol Bauer
Department of Electrical Sustainable Energy
Delft University of Technology
Mekelweg 4
Delft, the Netherlands
E-Mail: l.wang-11@tudelft.nl, z.qin-2@tudelft.nl, l.beloquilarumbe@tudelft.nl, p.bauer@tudelft.nl

Acknowledgements

This project has received funding from the Electronic Components and Systems for European Leadership Joint Undertaking under grant agreement No 876868. This Joint Undertaking receives support from the European Union's Horizon 2020 research and innovation programme and Germany, Slovakia, Netherlands, Spain, Italy.

Keywords

«Charging Infrastructure for EV's», «Power quality», «Modeling», «Harmonics».

Abstract

To accurately simulate the harmonic emission of EV DC fast chargers (DCFCs) and the harmonic voltage of the power grid to which the chargers are connected, a small time-step, i.e., typically smaller than 10μs, is required. However, for harmonic assessment, a long timescale, typically a day, is required. A conflict between accuracy and time efficiency exists. To address this issue, a multi-timescale modeling framework of fast charging stations (FCSs) is proposed in this paper. In the presented framework, the DCFCs' input impedance and harmonic current emission in the ideal grid condition, i.e., the grid impedance is zero and there are no background harmonic voltages, is obtained firstly through a converter switch model with a small timescale. Since the DCFC's input impedance and harmonic current source change in the charging course, the input impedance and harmonic emission at different input power should be obtained. Then, the DCFCs' input impedance and harmonic emission will be used in the fast-charging station modeling, where the DCFCs are simplified as their Norton equivalent circuits. In the station level modeling, a bigger time step, i.e., 1 minute, is used, since the DCFCs' operating power can be assumed as a constant in one minute. With this framework, the FCSs' long-term power quality performance can be assessed efficiently without neglecting the DCFCs' small timescale dynamics.

Introduction

For widespread EV adoption, the fast-charging station (FCS) is a crucial infrastructure which can alleviate EV customers' range anxiety for long-distance trips [1]. Therefore, many FSCs are planned to be installed or are under construction. However, there are several obstacles for the massive introduction of FCSs.

Among all the obstacles, one outstanding concern is the unclear power quality impact of the newly installed FCSs. A typical FCS is connected to the MV distribution grid and is equipped with several high-power DC fast chargers (DCFCs) and a battery energy storage system (BESS) [1], [2]. The DCFCs and the BESS are connected to the distribution grid with power converters. Hence, an FCS is essentially a power-electronic-based system, in a similar way to a wind farm or PV farm. In a power-

electronic-based system, there are risks of harmonic emission noncompliance and harmonic resonance [3]–[5]. Hence, such issues are also expected for FCSs.

For analyzing and estimating an FCS's potential harmonic issues, modeling and simulation of the FCS's harmonic performance is crucial. However, there is a challenge of making the simulation both accurate and time efficient [6]. On the one hand, a small timescale is needed for the harmonic simulation accuracy, since a typical DCFC use a high switching frequency, e.g., 20kHz and above. To simulate a DCFC's dynamics, simulation with a time step, typically less than 10us, is needed. On the other hand, the long-term observation of harmonics is needed for the power quality assessment. For instance, one of the indices that may be used for the harmonic assessment is the greatest 99% probability daily value of harmonic voltage components [7]. A simulation with small time step but for long-term evaluation is not practically feasible because of its high time and computational cost.

To address this simulation challenge, a multi-timescale modeling method is proposed for FCS's long-term harmonic evaluation. Two timescales, i.e., a small one for DCFC's dynamic simulation; and a large one for FCS's long-term harmonic simulation, are utilized. In the small timescale modeling, detailed design, e.g., circuit topology, modulation, current controller, and phase lock loop (PLL), of the DCFC are considered. Based on the detailed model, the DCFC's input impedance and harmonic current source at a certain operating power can be obtained. Then, in the large-timescale modeling, i.e., the FCS modeling, all the DCFCs can be simplified as their Norton equivalent circuit. Although each DCFC's input impedance and harmonic current source keep changing in its charging course, both can be assumed invariant in several minutes when there is no significant change of the DCFC's operating power. Hence, the simulation time step can increase to several minutes to improve the time efficiency.

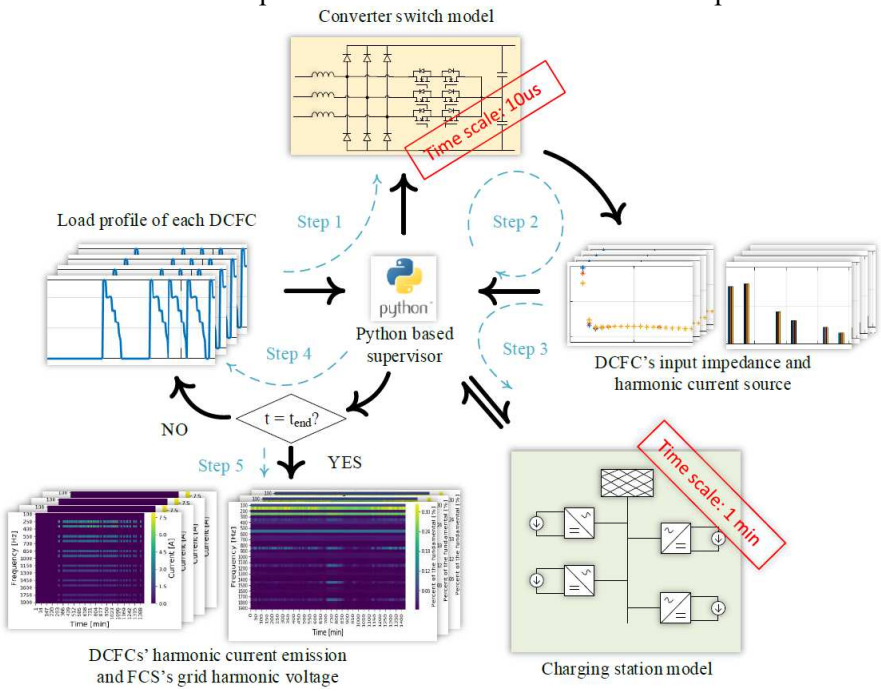

Fig. 1: Multi-timescale modeling framework of a fast-charging station for its power quality evaluation

The developed multi-timescale modeling framework is illustrated in Fig. 1. As shown in Fig. 1, at Step 1, the operating power $P_x(t_i)$ of each DCFC is obtained first, where $P_x(t_i)$ denotes the operating power of the DCFC x at time t_i. Then, at Step 2, the DCFCs' input impedance $Z_x(t_i, f_h)$ and harmonic current source $H_x(t_i, f_h)$ at time t_i and at all harmonic frequencies f_h are estimated with the small timescale simulation. Here, the harmonic frequencies selected are the integral multiples of the fundamental frequency in the range of 0 to 2 kHz. Later on, at Step 3, for the harmonic load flow simulation at t_i, each DCFC's input impedance and harmonic source in PowerFactory is updated to $Z_x(t_i, f_h)$ and $H_x(t_i, f_h)$ by Python. The simulation result of PowerFactory at t_i is sent to Python and recorded. Then, at Step 4, the time step is updated to t_{i+1}, and the aforementioned simulations are repeated. The iteration

continues until all the time steps in the load profile are finished. And in the final step, the simulation results are visualized.

In the following sections, the modeling of the DCFC and the FCS are presented first. Afterwards, the simulation results of the DCFC's input impedance and harmonic current source are presented. Then, a one-day load profile simulation with a time resolution of one minute is carried out to specify the DCFCs' operating points in that day. Later on, based on the developed FCS model and load profile, the FCS's long-term harmonic performance can be simulated by updating the DCFCs' input impedance and harmonic current source per minute.

Modeling of the DC fast charger

A typical DCFC comprises two power conversion stages, a front-end AC-to-DC stage, and a DC-to-DC stage. The two stages are buffered with a DC link where capacitors with large capacitance are used for a stable DC voltage level. Hence, the DCFC's impact on power quality is mainly determined by the front-end converter. As reported in [8], [9], Vienna Rectifier is one of the mainstream topology used for the DCFC's front-end converter, because of its superior performance on reliability, power density, and efficiency. Thus, Vienna Rectifier is selected for the DCFC to be modeled. Additionally, modular design is typical for DCFCs, especially for those with high-power rating, because of the 1) wide battery voltage range, 2) less stress on the power electronic components, 3) less design pressure on the cooling system, and 4) flexible compatibility with different EVs with different rated charging power [1]. Based on the selection of Vienna Rectifier and modular design concept, a 360-kW DCFC comprising twelve 30-kW parallel power modules is designed. The DCFC's 30-kW power module design is illustrated in Fig. 2. In Table I, the key parameters of the design are listed.

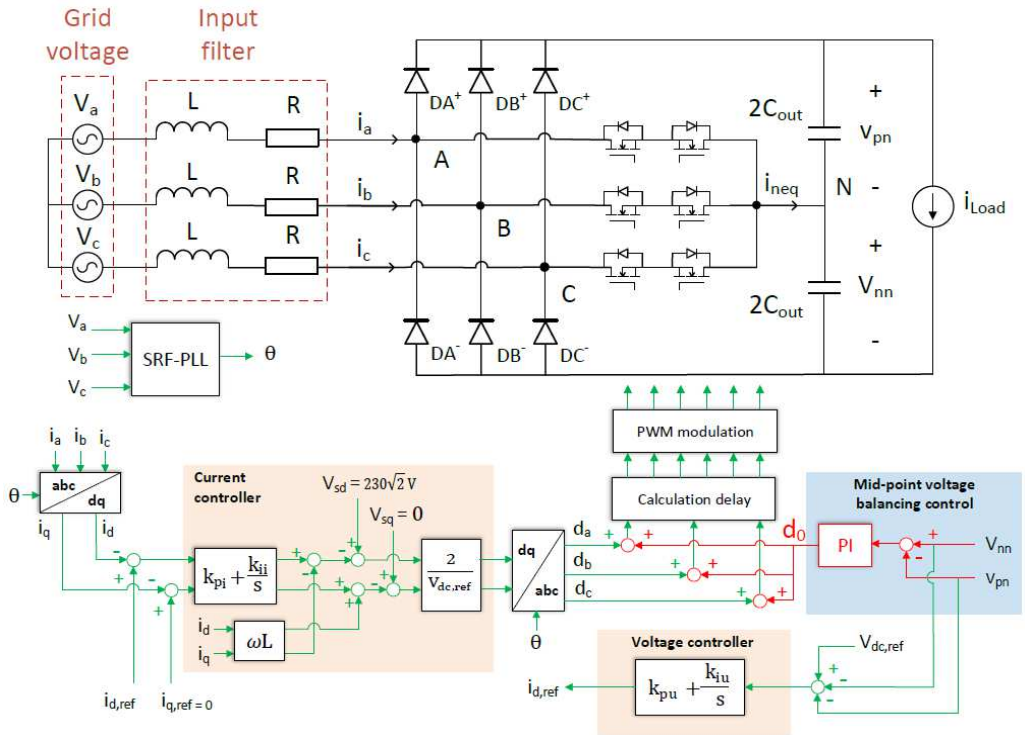

Fig. 2: The design of the DCFC's 30-kW power module

As shown in Fig. 2, the feedback control of the Vienna Rectifier comprises of current control, voltage control and mid-point voltage balancing control that ensure a small difference between V_{pn} and V_{nn}. The synchronous d-q frame PI controller [10] is used for current control. Additionally, the synchronous reference frame PLL (SRF-PLL) [10] is used to track the grid voltage phase. As digital control is used, a calculation delay of one switching cycle is included in the model. The pulse width modulation (PWM) [11], [12] signal is obtained with symmetrical modulation method, which updates

the duty cycle once per switching cycle. Therefore, the whole delay caused by the digital control roughly equals 1.5 T_{sw}, where T_{sw} is one switching cycle period.

Table I: The design parameters of the DCFC's 30-kW power module

Symbol	Description	Value	Symbol	Description	Value
V_a, V_b, V_c	line-to-neutral RMS voltage	230 V	BW_{PLL}	PLL bandwidth	100 Hz
C_{out}	Output capacitor capacitance	1.5 mF	L	Input filter inductance	250 μH
BW_{CL}	Current loop bandwidth	1 kHz	R	Input filter resistance	20 mΩ
BW_{VL}	Voltage loop bandwidth	400 Hz	f_{sw}	Switching frequency	20 kHz

Based on the DCFC's model shown in Fig. 2, the DCFC's harmonic current source at different operating power can be obtained, by monitoring the harmonic current of the input current . As for the input impedance, many analytic modeling for different applications have been published [10], [13], [14]. However, a simple approach to obtain the input impedance is using frequency sweep with either the switch model or real hardware. As illustrated in Fig. 3, the input impedance can be measured by injecting a small voltage perturbation V_h at the frequency f_h into the input 3-phase voltages. By measuring the harmonic component I_h at f_h in the input current, the input impedance at f_h can be calculated. It is worth noting that, depending on the sequence of the injected voltage perturbation, the measured input impedance is in the corresponding sequence domain, i.e., positive, or negative sequence domain. Since the frequency coupling impedance are much higher compared with their counterpart at f_h [10], they are neglected for simplicity.

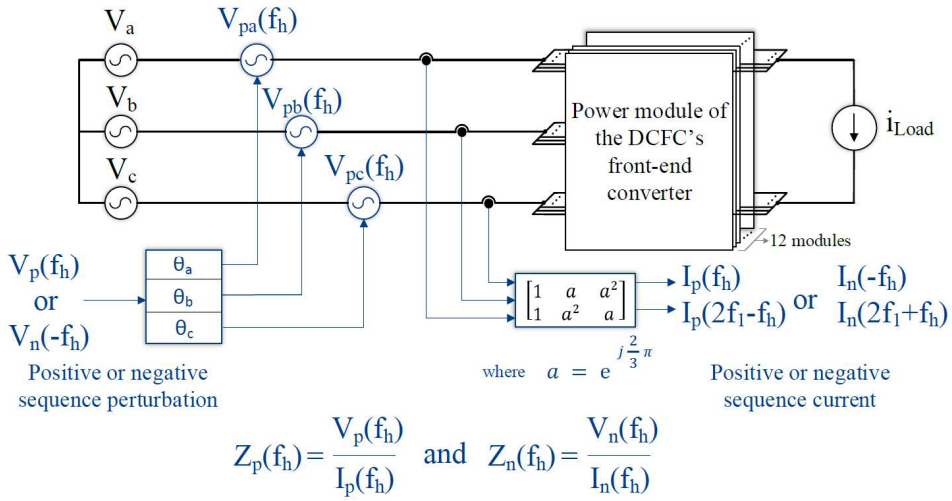

Fig. 3: The small voltage perturbation injection method for the DCFC's input impedance measurement

FCS's modeling

As illustrated in Fig. 4, an FCS with four 360-kW DCFCs is modeled. To fulfill the peak power demand with some margin, the service transformer has a capacity of 1.6 MVA. Additionally, since the FCS most likely constructed along the highway, a long distance between the substation and the FCS is expected. Therefore, the FCS is connected to the external grid with a low short circuit ratio (SCR), i.e., SCR equals 5, which indicates a weak grid condition.

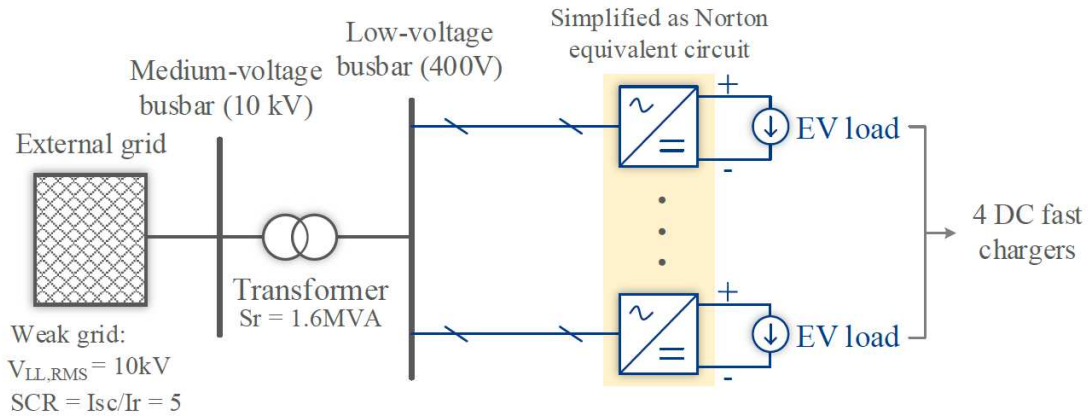

Fig. 4: The model of the fast-charging station with four 360-kW DCFCs in weak grid condition

As reported in [15], a typical MV grid voltage has a total harmonic distortion (THD) of 2%, which is averaged yearly. However, in some worst case, a THD of 4% is also observed. To explore the boundary condition for the occurrence of the FCS's power quality noncompliance, assumption of 4% THD for the grid voltage is used. The spectrum and time-domain waveform of the grid voltage are shown in Fig. 5, where it is worth noting that the harmonics of the assumed grid voltage are smaller than the recommended planning level in IEC 61000-2-12 [16].

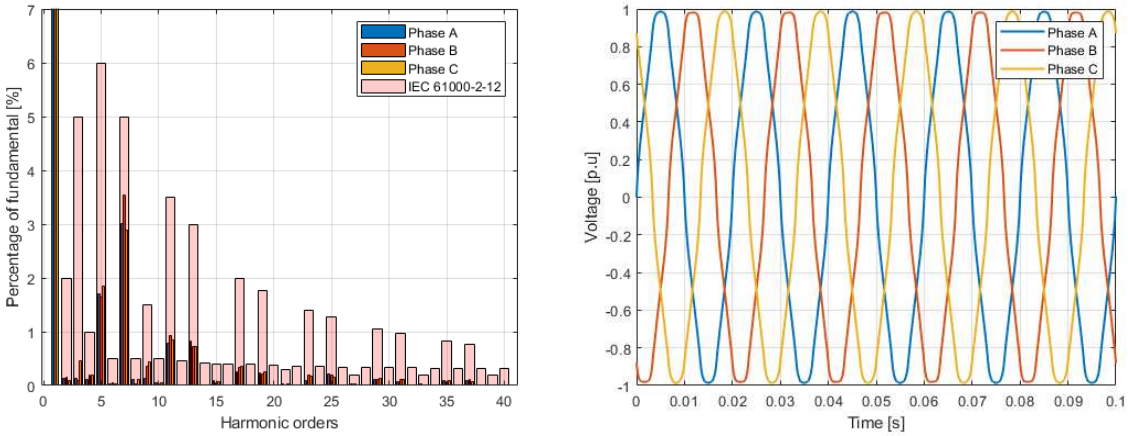

(a) (b)

Fig. 5: The (a) frequency spectrum and (b) time-domain waveform of the assumed grid voltage

At each simulation time step, the four DCFCs' input impedance and harmonic current source are updated according to their operating power at the time step to be simulated. Then, the harmonic load flow simulation in PowerFactory is carried out to evaluate the voltage harmonic at the low-voltage (LV) busbar and medium-voltage (MV) busbar. Such a modeling is also called quasi-dynamic modeling because the system dynamics within the simulation time step, i.e., one minute here, is ignored.

Simulation results and case study

A. The FCS's load profile

Based on the arrival time and the distribution of cars at a gasoline station in a day [17] and the charging profile of one EV [18], the load profile is generated by simply assuming that the state of charge (SoC) of each car equals 10% before charging and reaches 80% after finishing charging. The time resolution of the generated load profile is reduced to one minute by assuming the arrival time of cars has an even distribution in one hour. The resultant load profile is shown in Fig. 6.

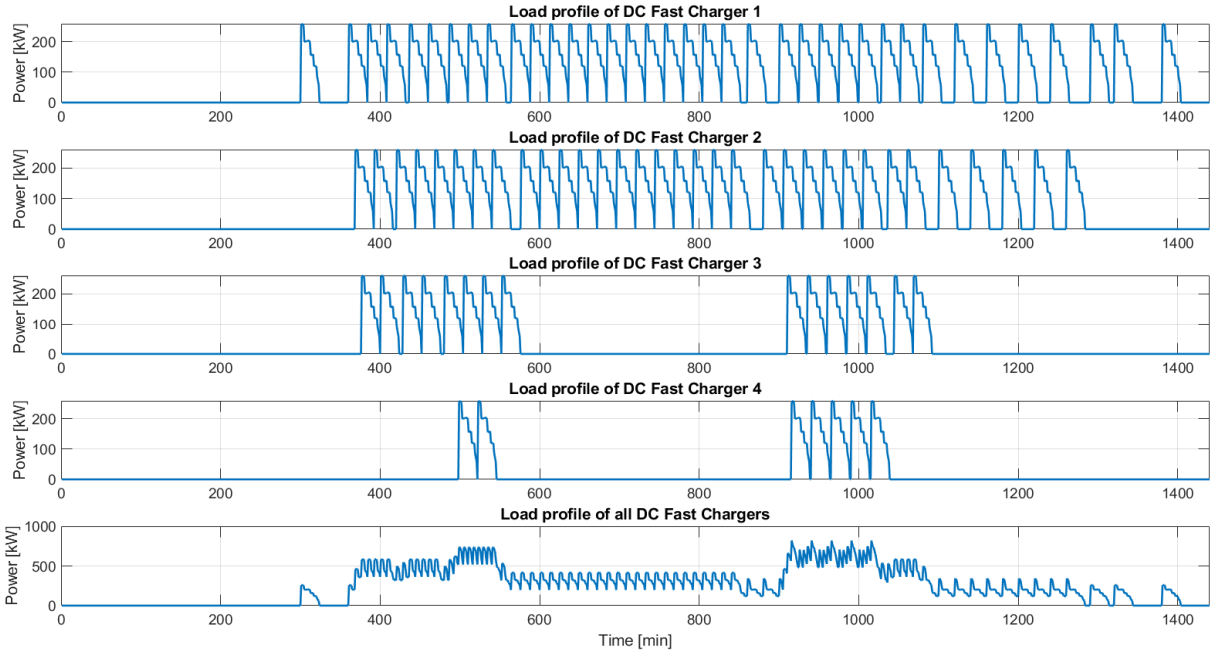

Fig. 6: The load profile of the fast-charging station

B. The DCFC's input impedance and primary harmonic emission

Based on the DCFC's model presented in Fig. 2 and the input impedance measurement method presented in Fig. 3, the DCFC's input impedance and harmonic current source at different operating powers (obtained from the load profile) are simulated. The simulation result shown in Fig. 7 compares the positive and negative sequence impedance of the DCFC at 260kW, 120kW, and 58kW, which are three operating powers in the load profile.

From Fig. 7, it is noted that the operating power has influence on the positive sequence impedance only for the frequencies smaller than 500 Hz. However, for the negative sequence impedance, the operating power has influence in the whole range of 100 Hz to 2 kHz. Due to the high switching frequency, and thereby the low delay induced by digital control, the negative resistance region in the impedance reported in [10] is not observed in the presented frequency range.

Additionally, the DCFC's input impedance is low because of the use of modular design. Since the power modules of a DCFC are connected in parallel, the input impedance of the DCFC is reduced.

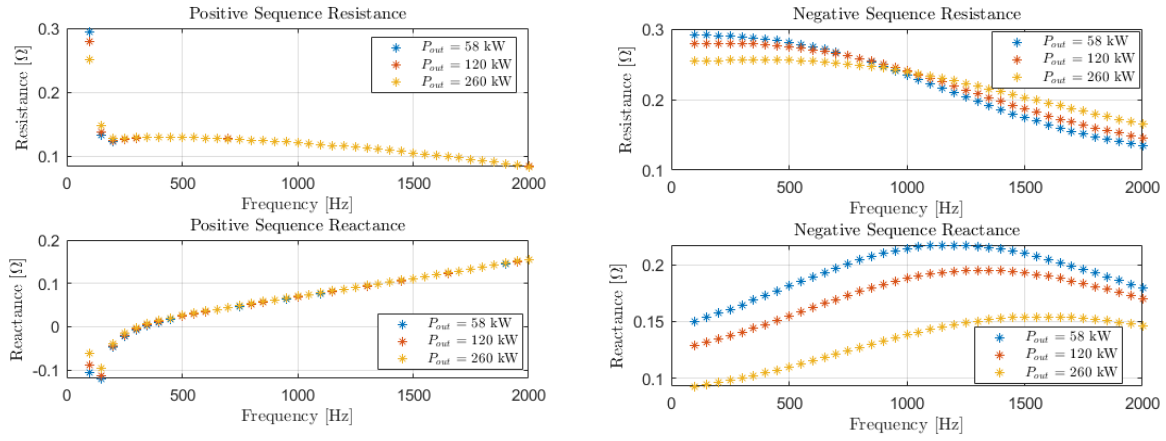

(a) (b)

Fig. 7: The DCFC's (a) positive sequence input impedance and (b) negative sequence input impedance at 260 kW, 120 kW, and 58 kW

In Fig. 8, the input current waveform and its spectrum of the DCFC at 260kW, 120kW, and 58kW are shown. From the results, it is noted that the difference among the DCFC's harmonic current source at different operating points are different from each other. Especially, the harmonic current is higher when the DCFC operates at low power. That is because, the control performance is worse when the input current is low.

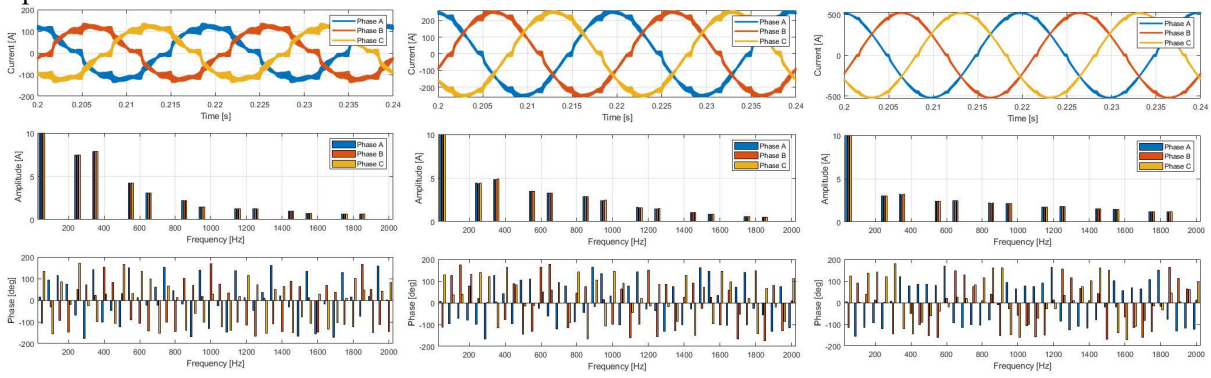

(a) (b) (c)

Fig. 8: The DCFC's harmonic current source when (a) the DCFC's input power is 58 kW; (b) the DCFC's input power is 120 kW; (c) the DCFC's input power is 260 kW

C. Quasi-Dynamic harmonic voltage and current simulation

After finishing the iteration of simulations for all time steps, the quasi-dynamic harmonic current emission of the DCFCs and the harmonic voltage in the FCS's network can be evaluated. The simulation results of the harmonic current emission of each DCFC are presented in Fig. 9. Each row in Fig. 9 contains 3 subfigures that show the real-time spectrum of one DCFC's three-phase input current. For instance, the subfigure at Row 1 and Column 1 with a title Char1_A shows the real-time spectrum of DCFC's Phase A input current.

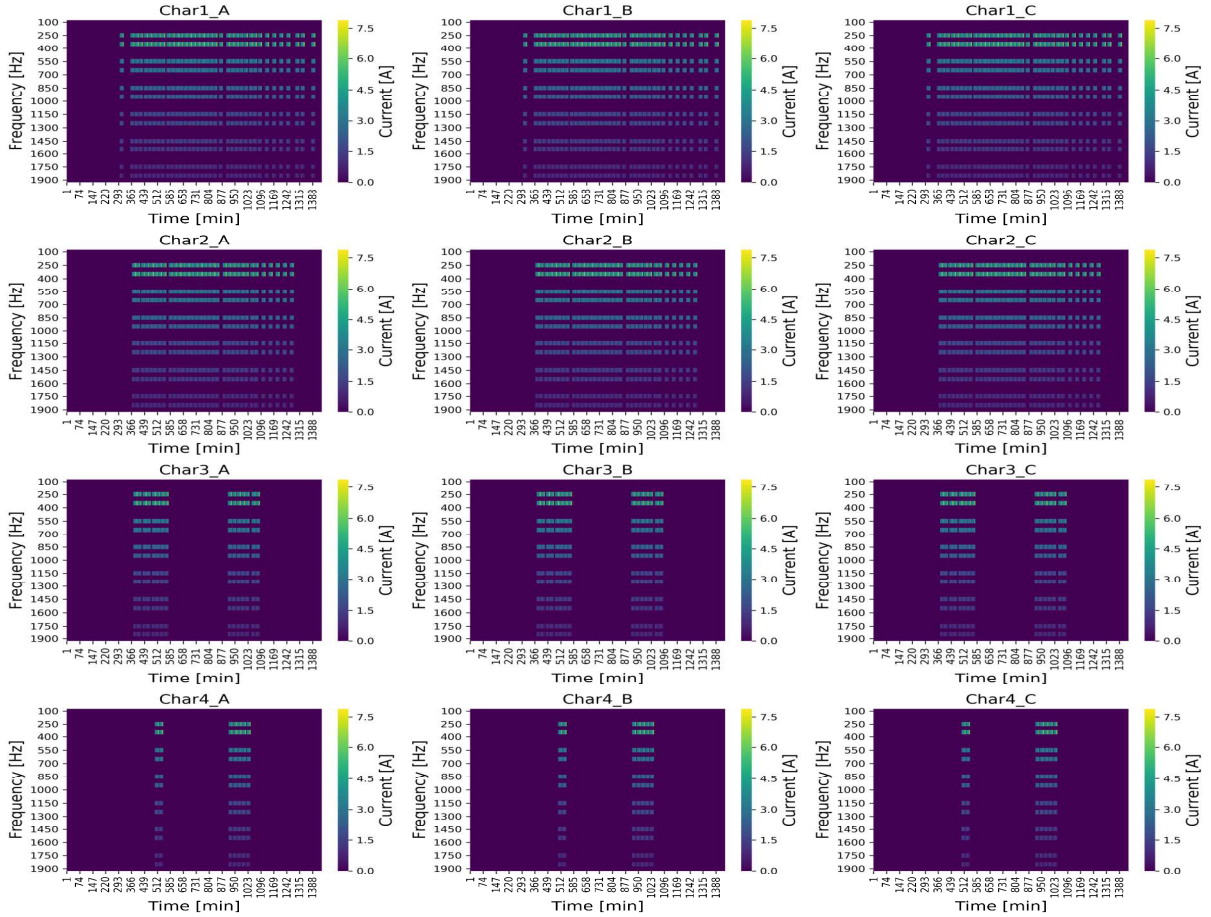

Fig. 9: The quasi-dynamic spectrum of the four DCFCs' three-phase input current. The title of the subfigure, e.g., CharX_P, denotes Phase P of DCFC X

The harmonic voltage of the three-phase voltages at the FCS's LV bus is shown in Fig. 10. As it is illustrated, the harmonic voltage at the FCS's LV bus is below the planning level shown in Fig. 5 in the whole day.

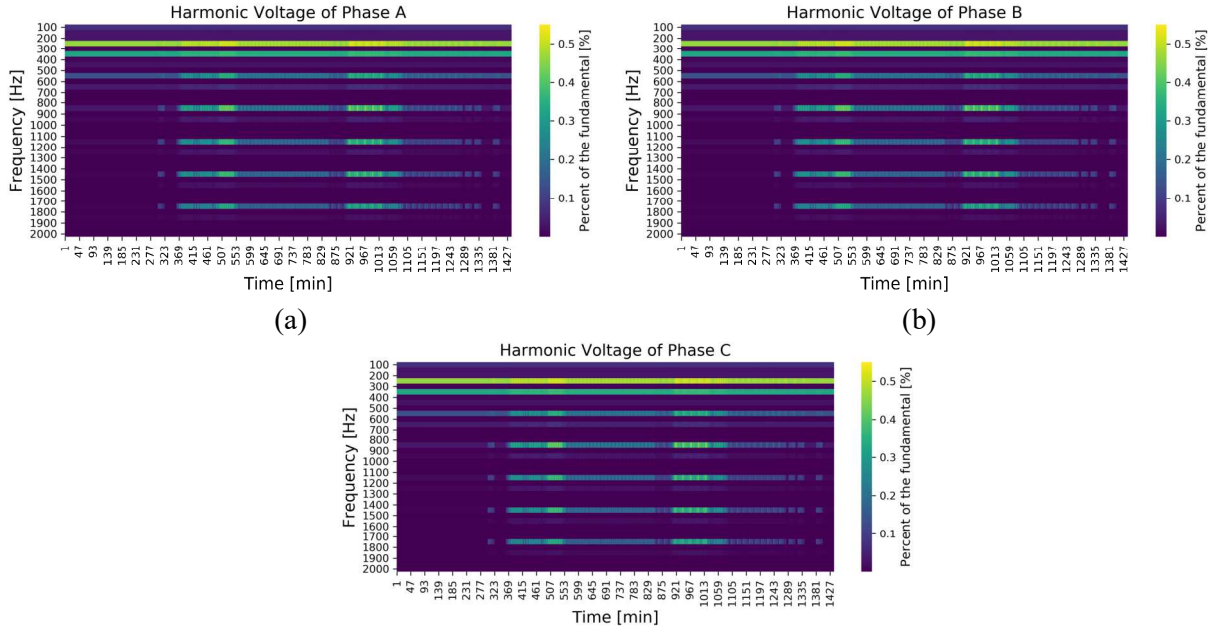

Fig. 10: The harmonic voltage of the (a) Phase A, (b) Phase B, and (c) Phase C of the FCS's LV bus voltage

As shown in Fig. 10, the simulated FCS's power quality is high, despite a high THD of the background harmonic voltage, which is mainly due to the DCFC's low input impedance. In particular, the DCFCs' harmonic current source, which is in parallel with the input impedance, will not induce high harmonic voltage distortion of the FCS's LV grid voltage. Moreover, a high grid impedance results in a low harmonic current flowing from the grid to the FCS. However, since in the simulation only 0-2kHz are selected, more research is needed to assess the risk of power quality issues.

Conclusion

A multi-timescale modeling method for an FCS for power quality analysis is presented. With the presented simulation framework, the real-time spectrum of the FCS's grid voltage and DCFCs' harmonic current emission in a long term can be evaluated time efficiently without neglecting the DCFC's small timescale dynamics. From the simulation results, it is revealed that the FCS's power quality compliance can be ensured in weak grid condition, since the DCFCs' input impedance is low and positive in all frequency range.

However, the simulation only evaluates the harmonic voltage, which is in the frequency range of 100 Hz to 2 kHz. It still lacks the evaluation for higher frequencies and interharmonics. Since the DCFCs' switching frequency is high, the negative input impedance induced by the digital control delay, might be observed at higher frequencies, which results in a risk of severe resonance and harmonic noncompliance. Based on the presented multi-timescale framework, future work will be carried out to evaluate the interharmonics and supraharmonics in the FCS's network.

References

[1] L. Wang, Z. Qin, T. Slangen, P. Bauer, and T. van Wijk, "Grid Impact of Electric Vehicle Fast Charging Stations: Trends, Standards, Issues and Mitigation Measures - An Overview," *IEEE Open Journal of Power Electronics*, vol. 2, pp. 56–74, 2021, doi: 10.1109/OJPEL.2021.3054601.
[2] S. Srdic and S. Lukic, "Toward Extreme Fast Charging: Challenges and Opportunities in Directly Connecting to Medium-Voltage Line," *IEEE Electrification Magazine*, vol. 7, no. 1, pp. 22–31, Mar. 2019, doi: 10.1109/MELE.2018.2889547.
[3] J. H. R. Enslin and P. J. M. Heskes, "Harmonic interaction between a large number of distributed power inverters and the distribution network," *IEEE Transactions on Power Electronics*, vol. 19, no. 6, pp. 1586–1593, Nov. 2004, doi: 10.1109/TPEL.2004.836615.
[4] L. Beloqui Larumbe, Z. Qin, and P. Bauer, "Introduction to the Analysis of Harmonics and Resonances in Large Offshore Wind Power Plants," in *2018 IEEE 18th International Power Electronics and Motion Control Conference (PEMC)*, Aug. 2018, pp. 393–400. doi: 10.1109/EPEPEMC.2018.8521974.
[5] J. Lei, Z. Qin, W. Li, P. Bauer, and X. He, "Stability Region Exploring of Shunt Active Power Filters Based on Output Admittance Modeling," *IEEE Transactions on Industrial Electronics*, pp. 1–1, 2020, doi: 10.1109/TIE.2020.3044750.
[6] L. Wang, Z. Qin, J. Dong, and P. Bauer, "Design, modelling and evaluation of a GaN based motor drive for a solar car," in *IECON 2019 - 45th Annual Conference of the IEEE Industrial Electronics Society*, Oct. 2019, vol. 1, pp. 5120–5125. doi: 10.1109/IECON.2019.8927042.
[7] *Electromagnetic compatibility (EMC) - Part 4-7: Testing and measurement techniques - General guide on harmonics and interharmonics measurements and instrumentation, for power supply systems and equipment connected thereto*, IEC Std. 61000-4-7, 2009.
[8] S. Chon, M. Bhardwaj, and H. Nene, "Maximizing power for Level 3 EV charging stations," 2018.
[9] "Tackling the Challenges of Electric Vehicles Fast Chargings." Accessed: Jun. 16, 2020. [Online]. Available: https://www.infineon.com/dgdl/Infineon-Tackling_the_Challenges_of_Electric_Vehicles_Fast_Chargings-Article-v01_00-EN.pdf?fileId=5546d4626eab8fbf016f0c5d34f442fc
[10] M. Cespedes and J. Sun, "Impedance Modeling and Analysis of Grid-Connected Voltage-Source Converters," *IEEE Transactions on Power Electronics*, vol. 29, no. 3, pp. 1254–1261, Mar. 2014, doi: 10.1109/TPEL.2013.2262473.
[11] J. Xu, J. Han, Y. Wang, S. Habib, and H. Tang, "A Novel Scalar PWM Method to Reduce Leakage Current in Three-Phase Two-Level Transformerless Grid-Connected VSIs," *IEEE Transactions on Industrial Electronics*, vol. 67, no. 5, pp. 3788–3797, May 2020, doi: 10.1109/TIE.2019.2920597.
[12] J. Xu, J. Han, Y. Wang, M. Ali, and H. Tang, "High-Frequency SiC Three-Phase VSIs With Common-Mode Voltage Reduction and Improved Performance Using Novel Tri-State PWM Method," *IEEE Transactions on Power Electronics*, vol. 34, no. 2, pp. 1809–1822, Feb. 2019, doi: 10.1109/TPEL.2018.2829530.
[13] L. B. Larumbe, Z. Qin, and P. Bauer, "On the Importance of Tracking the Negative-Sequence Phase-Angle in Three-Phase Inverters with Double Synchronous Reference Frame Current Control," in *2020 IEEE 29th International Symposium on Industrial Electronics (ISIE)*, Jun. 2020, pp. 1284–1289. doi: 10.1109/ISIE45063.2020.9152442.
[14] L. B. Larumbe, Z. Qin, and P. Bauer, "Output Impedance Modelling and Sensitivity Study of Grid-Feeding Inverters with Dual Current Control," in *IECON 2019 - 45th Annual Conference of the IEEE Industrial Electronics Society*, Oct. 2019, vol. 1, pp. 4007–4012. doi: 10.1109/IECON.2019.8927067.
[15] "Spanningswkaliteit in Nederland 2014," Movares Nederland B.V., RMI-LD-140016509 / Versie 1.2. Accessed: May 26, 2021. [Online]. Available: https://www.vemw.nl/~/media/VEMW/Downloads/Public/Elektriciteit/Spanningswkaliteit%20in%20Nederland%202014.ashx
[16] *Electromagnetic compatibility (EMC) - Part 2-12: Environment - Compatibility levels for low-frequency conducted disturbances and signalling in public medium-voltage power supply systems,* IEC Std. 61000-2-12, 2003.
[17] K. Yunus, H. Z. De La Parra, and M. Reza, "Distribution grid impact of Plug-In Electric Vehicles charging at fast charging stations using stochastic charging model," in *Proceedings of the 2011 14th European Conference on Power Electronics and Applications*, Aug. 2011, pp. 1–11.
[18] "Charging with a Porsche Taycan," *Fastned support*. https://support.fastned.nl/hc/en-gb/articles/360039667693-Charging-with-a-Porsche-Taycan (accessed Feb. 23, 2021).